ISSN 1063-7745, Crystallography Reports, 2019, Vol. 64, No. 1, pp. 16–23. © Pleiades Publishing, Inc., 2019.
Russian Text © V.G. Kohn, 2019, published in Kristallografiya, 2019, Vol. 64, No. 1, pp. 20–28.

## DIFFRACTION AND SCATTERING OF IONIZING RADIATIONS

# Theory of Two-Beam X-Ray Diffractometry Method Using Synchrotron Radiation

**V. G. Kohn**[a,b]

[a] *National Research Centre "Kurchatov Institute," Moscow, 123182 Russia*

[b] *Shubnikov Institute of Crystallography, Federal Scientific Research Centre "Crystallography and Photonics," Russian Academy of Sciences, Moscow, 119333 Russia*

*e-mail: kohnvict@yandex.ru*

Received September 27, 2017; revised September 27, 2017; accepted November 23, 2017

**Abstract**—An accurate theory of the new method of two-beam X-ray diffractometry using synchrotron radiation has been developed. In this method, a beam from the source is reflected from two monochromator crystals without changing direction and then is collimated by a slit with a relatively small size. A diffraction reflection curve (DRC) is obtained by recording the integrated intensity during crystal sample rotation near the Bragg angle for a certain energy, specified by the monochromator. The theory accurately takes into account the influence of the source sizes, the distances, and the slit size on the formation of experimental DRC. It is shown that a practically intrinsic DRC of crystal sample can be obtained even for symmetric reflections from the monochromator crystals and crystal sample if the Bragg angle in the monochromator crystals exceeds the Bragg angle in the crystal sample by a factor of 2 or more. The slit size should to be optimized to exclude its influence on the DRC.

**DOI:** 10.1134/S1063774519010127

## INTRODUCTION

Laboratory studies of X-ray diffraction in crystals have been performed for many years in two complementary schemes, referred to "X-ray section topography" and "double-crystal X-ray diffractometry" [1]. An X-ray tube forming a quasi-monochromatic beam was used as a source. However, the spectral FWHM (full width at half maximum) of X-ray tube characteristic radiation is insufficiently small to implement a necessary temporal coherence. At the same time, a relatively large emitting surface area corresponds to a small spatial coherence length.

In the case of X-ray section topography, a coherent beam is formed by placing a narrow slit before the crystal [2], which limits the beam spatial sizes. As was shown in [3], under these conditions a slit becomes a secondary incoherent source; since this source is small in size, one can observe (on a photographic film) large-period interference fringes in the central region of irradiated area, which are described by the diffraction theory of spherical waves [4].

In double-crystal X-ray diffractometry, the problem of forming a coherent beam is solved differently. The area-integrated intensity after the reflection from two crystals is measured as a function of the rotation angle of the second crystal relative to the first one. First and second crystals are referred to as monochromator and sample, respectively. Using a nondispersive scheme (in which the Bragg angles in both crystals coincide) and asymmetric reflection from the monochromator, one can obtain a practically intrinsic diffraction reflection curve (DRC), which coincides with the theoretical angular dependence of reflection intensity in the case of diffraction of a plane monochromatic wave [1].

When such experiments are carried out with a synchrotron radiation (SR) source, several new problems arise. First, the use of a nondispersive scheme and asymmetric reflection from monochromator is not always possible and desirable. At the same time, the SR spectrum is very wide, and it is necessary to limit it additionally for the following reason: the first crystal operates as a prism, converting a frequency spectrum into an angular spectrum, because the Bragg angle depends almost linearly on frequency in a narrow frequency range.

Generally, two pairs of crystals in the dispersion scheme are used to form an almost parallel and monochromatic SR beam (see, e.g., [5, 6]). Two crystals must be used for each reflection to retain the beam direction.

In the SR experiment performed in [7], a narrow slit was installed before the crystal sample in addition to the symmetric monochromator, consisting of a pair of crystals. The three-beam coplanar diffraction in paratellurite ($TeO_2$) was investigated. It is convenient

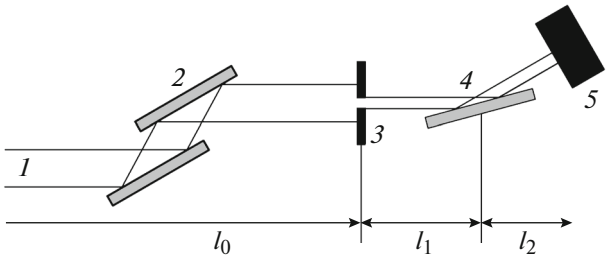


**Fig. 1.** Schematic of the experiment: (*1*) SR beam, (*2*) monochromator, (*3*) slit, (*4*) crystal sample, and (*5*) detector.

to use SR in such experiments, because the monochromator makes it possible to select any radiation frequency and thus construct a two-dimensional (angle–frequency) map, in which multibeam interaction can easily be observed.

However, it turned out that the two-beam DRCs, both for strong (with small Miller indices) and weak (with large Miller indices) reflections, had a FWHM greatly exceeding that of the intrinsic DRCs; and the weak-reflection broadening was much larger. Similar experimental results obtained in [8] with a laboratory radiation source could readily be modeled within the existing theory.

Moreover, recent experiments using SR in the aforementioned scheme [9] of measuring two-beam DRCs in silicon for different indices of reflections from monochromator and sample and different slit sizes showed some interesting features. To explain them, a more accurate theory should be developed, which would explicitly take into account all characteristics of the experimental scheme, including not only the crystal parameters but also the source size, the distance to the slit installed before the crystal sample, and the slit size.

Some attempts to describe theoretically experimental schemes with a possibility of numerical simulation of experiment have been made previously (see, e.g., [5, 10–12]); however, the versions in which both the diffraction in the crystal and the diffraction from the slit must be simultaneously and accurately taken into account have not been considered.

This study presents a successive theory, which accurately takes into account for the first time the source size, the diffraction in the crystals and from the slit, and the distances between the optical scheme elements. The calculation was performed from first principles, using the methods developed when calculating phase-contrast images of noncrystalline objects, with limitations imposed on the spatial and temporal coherence, and the diffraction of spatially inhomogeneous beams (see, e.g., [13–15]).

The general formula turned out to be rather complicated for analysis; however, the use of two approximations (small and large slit sizes) made it possible to derive formulas convenient for numerical calculation; some physical conclusions can also be drawn based on these formulas.

## STATEMENT OF THE PROBLEM

A schematic diagram of the experiment is shown in Fig. 1. The experimental setup consists of an SR source, a double-crystal monochromator, a slit, a crystal sample, and a detector. SR is known to be generated when electrons are decelerated in a cloud during its circular motion. Different electrons release short wave trains at different instants; therefore, their radiation is phase-incoherent. A good approximation of this source is a set of point sources that are located in a plane perpendicular to the beam direction and have a white emission spectrum [15].

Different frequencies in the emission spectrum are incoherent for the same reason. The detector records a large set of short trains from each source point. They are time-incoherent, and the measurement time significantly exceeds the duration of individual trains [16]. Therefore, the Maxwell equations must be solved for a point monochromatic source. In the first stage, the integrated radiation intensity recorded by the detector is calculated. Then the intensity is summed over the spectrum and over point coordinates on the source, with allowance for the intensity of individual points.

It is necessary to calculate the dependence of the integrated intensity on the crystal sample rotation angle and understand how the monochromator, slit size, and source angular size affect this intensity. The slit can be described only in real space relative to the basic coordinate system; for this reason, the calculation begins in real space.

Let us consider the wave function of the monochromatic component of radiation with a specified frequency. We choose an arbitrary point (with a coordinate $x_s$) on the intersection line between the source cross section and diffraction plane and the basic trajectory (coordinate system), which begins at this point and goes parallel to the $z$ axis. At the point where it reaches the surface of the first monochromator crystal, it deviates by the double Bragg angle, corresponding to the basic radiation frequency, and goes in a new direction to the second crystal. Then it deviates again by the same angle but to the opposite side and goes (again parallel to the $z$ axis) to the slit.

In the case of two-beam diffraction, the wave function of radiation changes only in the diffraction plane, which is formed by the beam propagation direction and the reciprocal lattice vector (the latter characterizes the set of atomic planes this beam reflects off). In the perpendicular plane, the crystals in no way distort the beam; hence, this plane can be disregarded.

The amplitude of the X-ray electric field of specified polarization before the slit can be written in the form $\exp(iKz)A_0'(x,q_1)$, where $K = \omega/c = 2\pi/\lambda$ is the wave number, $\omega$ is the radiation frequency, $c$ is the speed of light, and $\lambda$ is the wavelength. This amplitude can be presented as a superposition of plane waves by writing the function $A_0'(x,q_1)$ in the form of a Fourier integral:

$$A_0'(x,q_1) = \int \frac{dq}{2\pi} \exp(iqx) P_M^2(q - q_1) P(q, l_0). \quad (1)$$

Here, $q$ is the modulus of a component of the wave vector $\mathbf{k}_0 = \mathbf{K}_0 + \mathbf{q}$ for a plane wave in the diffraction plane along a direction perpendicular to the trajectory. The wave vector component $\mathbf{K}_0$ along the trajectory exactly satisfies the Bragg condition for the basic frequency and yields an additional phase factor. This factor does not affect the intensity and, therefore, is omitted from here on. The vector $\mathbf{q}$ is directed so as to make an obtuse angle with the reciprocal lattice vector $\mathbf{h}$.

A reflection from crystal transforms the wave vector $\mathbf{k}_0$ into the wave vector $\mathbf{k}_h = \mathbf{K}_h + \mathbf{q}_h$, where $\mathbf{K}_h = \mathbf{K}_0 + \mathbf{h}$, and the vector $\mathbf{q}_h$ differs from $\mathbf{q}$ by a component parallel to the normal to the crystal surface, which is antiparallel to the reciprocal lattice vector in the case of symmetric Bragg reflection. The modulus of this component is found from the condition $\mathbf{K}_h\mathbf{q}_h = 0$ (i.e., $\mathbf{q}_h$ is perpendicular to $\mathbf{K}_h$). It can be shown that, in the case of symmetric diffraction, the modulus of vector $\mathbf{q}_h$ is equal to $q$ and has a correct direction. In other words, the plane wave direction is completely retained under conditions of double reflection.

The wave vector is transformed in this way when radiation emerges from a crystal because of the refraction at the crystal boundary. The reason is that the wave vector modulus cannot change in air, provided that the radiation frequency remains constant. The wave vector in the crystal is different: it is equal to $\mathbf{k}_h' = \mathbf{K}_h + \mathbf{q}$, and its modulus differs from that of the initial vector $\mathbf{k}_0$. Correspondingly, the parameter characterizing the deviation from the Bragg condition is $\alpha = ((\mathbf{k}_0 + \mathbf{h})^2 - K^2)/K^2 = 2\mathbf{hq}/K^2$.

Formula (1) directly takes into account that the Fourier transform of the Fresnel propagator

$$P(q,z) = \exp\left(-i\frac{\lambda z}{4\pi}q^2\right) \quad (2)$$

depends on the total distance $l_0$ along the basic trajectory. In fact, one should write the product of three propagators: to the first crystal, between the crystals, and after the second crystal. However, the explicit form of function (2) suggests that the product is equal to the new propagator at the total distance.

The Fresnel propagator is a part of spherical wave in the paraxial approximation, with the basic plane wave in the beam direction disregarded. The convolution of the wave function and propagator describes the radiation propagation in air. The diffraction reflection amplitudes (DRAs) for two monochromator crystals are also multiplied, which yields a squared DRA for one crystal, $P_M(q)$, because the crystals are identical. The crystals, being oriented arbitrarily, operate efficiently only at the frequency for which the Bragg angle corresponds to the basic trajectory passing through the middle of the slit. This frequency is the basic one.

Let us consider a limited and relatively narrow frequency range in the vicinity of the basic frequency. In the case of arbitrary deviation of radiation frequency from the basic value, the Bragg conditions for the monochromator crystals are not satisfied exactly at $q = 0$. However, at a small variation in frequency, the frequency dependence of the diffraction parameters can be neglected. Concerning the deviation from the Bragg condition, it can be compensated for by rotating the crystals at the same angle: $\theta_1 = q_1/K$.

To determine this angle, we will write the Bragg condition in the form $2d\sin(\theta_{B1} + \theta_1) = \lambda + \Delta\lambda$, where $d$ is the interplanar spacing in crystal, $\theta_{B1}$ is the Bragg angle for the basic frequency, and $\lambda$ is the basic wavelength. Hence, we find approximately that $\theta_1 = (\Delta\lambda/\lambda)\tan\theta_{B1} = -(\Delta\omega/\omega)\tan\theta_{B1}$.

The Fresnel propagator should depend on the real radiation frequency. However, a small relative change in frequency can be compensated for by a small relative change in distance, although the result is known to depend only slightly on a small variation in distance. In other words, the basic frequency value can be used. As a result, the change in radiation frequency is efficiently determined by only the parameter $q_1$.

The wave function behind the slit is obtained multiplying function (1) by the slit transmission function $T(x)$:

$$A_1'(x, x_s, q_1) = A_0'(x, q_1)T(x + x_s), \quad T(x) = \theta(x_0 - |x|). \quad (3)$$

Here, $\theta(x)$ is the Heaviside step function, which is equal to unity and zero for positive and negative arguments, respectively, and $x_0$ is the slit half width. With a change in the coordinate $x_s$ of radiation source point, the basic trajectory shifts at the same distance. The slit center shifts at the same distance in the opposite direction with respect to it. It is assumed that the basic trajectory passes through the slit center at the coordinate $x_s = 0$; i.e., the slit position must be optimized with respect to the source position.

To solve the problem, one should present function (3) as a superposition of plane waves,

$$A_1'(x, x_s, q_1) = \int \frac{dq}{2\pi} \exp(iqx) A_1(q, x_s, q_1), \quad (4)$$

i.e., calculate the inverse Fourier transform:

$$A_1(q, x_s, q_1) = \int dx \exp(-iqx) A_1'(x, x_s, q_1). \quad (5)$$

Finally, the wave function on the detector is determined by the integral

$$A_2'(x, x_s, q_1, \theta_r) = \int \frac{dq}{2\pi} \exp(iqbx) P_C(q_r + q_2 - q) \times P(q, l_1) P(qb, l_2) A_1(q, x_s, q_1), \quad (6)$$

where $l_1$ is the distance from the slit to the crystal sample, $l_2$ is the distance from the crystal sample to the detector, and $P_C(q)$ is the crystal sample DRA.

This formula takes into account two specific features of crystal sample reflection. The first is that the crystal sample can be rotated; therefore its DRA is counted from the angle $\theta_r = q_r/K$ of crystal rotation with respect to the position at which the reflection is maximum for the basic frequency. A change in frequency gives rise to an additional rotation angle, in the same way as it is taken into account in the monochromator: $q_2 = K\theta_2$, $\theta_2 = (\Delta\lambda/\lambda)\tan\theta_{B2}$.

It is important that $q_2 = q_1 M$, where $M = \tan\theta_{B2}/\tan\theta_{B1}$. The opposite sign of the argument of the crystal sample DRA function is explained by the fact that the crystal sample is oriented not parallel to the monochromator crystals but makes the angle $\pi - \theta_{B1} - \theta_{B2}$ with them. The first monochromator crystal reflects the horizontal beam upwards, whereas the crystal sample reflects it downwards.

The second feature is that the reflection in the crystal sample may be asymmetric; i.e., the normal to the crystal surface is not antiparallel to the reciprocal lattice vector. The crystal changes not only the direction of the beam but also its angular divergence.

It is generally assumed that the DRA argument is the angular deviation of entering beam: $\theta = q/K$. However, the angular deviation with respect to the basic trajectory at the crystal output is $\theta' = qb/K$, where $b = \sin\theta_0/\sin\theta_h$; $\theta_{0,h}$ are acute angles formed by the wave vectors $\mathbf{K}_{0,h}$ with the crystal surface [1]. Note that $\theta_0 + \theta_h = 2\theta_B$. In the symmetric case, $\theta_0 = \theta_h = \theta_B$.

The integrated intensity recorded by detector is measured as a function of crystal rotation angle $\theta_r$ in an experiment. Correspondingly, we derive the following relation from (6):

$$S_1(\theta_r, x_s, q_1) = \int dx |A_2'(x, \theta_r, x_s, q_1)|^2 = b^{-1} \int \frac{dq}{2\pi} |P_C(q_r + q_2 - q)|^2 |A_1(q, x_s, q_1)|^2. \quad (7)$$

The factor $b^{-1}$, provided that it differs from unity, is only a manifestation of the fact that the variables $x$ and $q$ are not complementary. The coordinate $q$ in the reciprocal space corresponds to the coordinate $xb$ on the detector.

Formula (7) is the well-known Parseval rule, according to which the integrals over intensity in the real and reciprocal spaces are equal. Since the modulus of the Fresnel propagator Fourier transform is unity, the crystal–detector distance does not affect the integrated intensity. This is a consequence of the general law of energy conservation.

To perform a comparison with experiment, it is necessary to calculate the integral of this function over the source size and emission spectrum. As a result, we arrive at the function of crystal rotation angle, which is generally referred to as DRC. It is determined by the formula

$$S(\theta_r) = \int dx_s G_B(x_s) \int \frac{dq_1}{2\pi} S_1(\theta_r, x_s, q_1), \quad (8)$$

where $G_B(x_s)$ is the function of source intensity at the point $x_s$, which is generally approximated by a Gaussian. In the general case, the problem appears to be fairly complex; however, there are limiting cases, in which simpler approximate formula can be obtained.

For simplicity, we will omit below the factors that do not affect the DRC shape. Concerning the maximum value, theoretical calculations are generally performed using a normalization constant that yields the intrinsic DRC of crystal sample in the most favorable case. When comparing with experiment, the constant factor is a fitting parameter.

## INFLUENCE OF THE SLIT SIZE ON DRC

To calculate the function $A_1(q, x_s, q_1)$, let us substitute formulas (1) and (3) into (5) and shift the origin of coordinates in the integral over $x$. As a result, we arrive at

$$A_1(q, x_s, q_1) = \int dx T(x) \int \frac{dq'}{2\pi} P_M^2(q' - q_1) P(q', l_0) \times \exp(i[q' - q][x - x_s]). \quad (9)$$

The integrand contains a rapidly oscillating exponential function. To estimate approximately the integral, we will apply the stationary-phase method for the integral over $q'$ in the integral over $x$.

The exponential argument (phase) and the stationary-phase point are given, respectively, by the formulas

$$\varphi(q') = -r^2 q'^2/2 + q'(x - x_s), \quad q' = q_x + q_s, \quad (10)$$

where

$$r^2 = \frac{\lambda l_0}{2\pi} = \frac{l_0}{K}, \quad q_x = \frac{x}{r^2}, \quad q_s = -\frac{x_s}{r^2}. \quad (11)$$

The stationary-phase method implies integration of the exponential, whereas the other parts of the integrand are taken outside the integral at the stationary-phase point.

As a result, we have an approximate formula

$$A_1(q, x_s, q_1) \propto \int dx T(x) P_M^2(q_x + q_s - q_1) \times \exp\left( i \frac{x^2}{2r^2} - i[q - q_s]x \right). \quad (12)$$

The phase factor is omitted here (because we are interested in only the modulus of this expression), as well as the constant factor, which is independent of the function arguments.

In the general case, one must calculate integral (12), which depends efficiently on two independent arguments: $(q_s - q_1)$ and $(q - q_s)$. To obtain a simpler solution, we will consider two limiting cases.

In the first case, the slit has a very small size. The variable $q_x$ in the argument of function $P_M^2$ and the term quadratic in $x$ in the exponential argument can be neglected because of their smallness. As a result, the formula takes a simpler form:

$$A_1(q, x_s, q_1) \propto P_M^2(q_s - q_1)F(q - q_s), \tag{13}$$

where

$$F(q) = \int dx \exp(-iqx)T(x) = \frac{2}{q}\sin(qx_0). \tag{14}$$

The second case is a slit of very large size. The presence of a term quadratic in the coordinate $x$ in the exponential becomes important; it indicates that the slit does not contribute entirely to the integral: some of its regions are more efficient than others. We apply again the stationary-phase approximation, but now to the integral over $x$. The stationary-phase point coordinate is $x = r^2(q - q_s)$. Correspondingly, $q_x = q - q_s$ at this point; having made a substitution, we arrive at a simpler formula:

$$\left|A_1(q, x_s, q_1)\right|^2 \propto T(r^2[q - q_s])\left|P_M^2(q - q_1)\right|^2. \tag{15}$$

The analysis of theoretical formulas is significantly simplified in both limiting cases. Concerning the range of their applicability, an evident condition for the first case is the inequality $x_0 < r$. Its physical meaning is that the slit size should to be sufficiently small to neglect the curvature of the constant-phase surface of spherical wave in the slit region. In other words, the incident radiation before the slit is very similar to a plane wave, whose direction depends on the point source coordinate $x_s$.

Obviously, the inverse inequality $x_0 \gg r$ must be valid in the second limiting case. Concerning the conditions for the width of the intrinsic DRCs of the monochromator and crystal sample, this problem is more complex. It can be solved either performing numerical experiments or comparing with the results of real experiments.

## LIMITING CASE OF SMALL-SIZE SLIT

In this case, we obtain the following approximation for experimental DRC by passing from integration variable $x_s$ to variable $q_s$:

$$S(\theta_r) \propto \int \frac{dq_s}{2\pi} G_B(q_s) \int \frac{dq_1}{2\pi} G_M(q_s - q_1) \times \int \frac{dq}{2\pi} G_C(q_r + q_1 M - q) G_s(q - q_s), \tag{16}$$

where

$$G_M(q) = \left|P_M^2(q)\right|^2, \quad G_C(q) = \left|P_C(q)\right|^2, \quad G_s(q) = \left|F(q)\right|^2. \tag{17}$$

It is convenient to calculate a triple integral using Fourier integrals of the functions

$$G_{B,M,C,S}(q) = \int dx G'_{B,M,C,S}(x) \exp(-iqx). \tag{18}$$

Substituting (18) into (16), we obtain a sevenfold integral, in which three integrals over $q$ are three delta functions, which take off three more integrals over $x$; as a result, we have

$$S(\theta_r) \propto \int dx G'_B([1 - M]x) G'_M(Mx) \times G'_C(x) G'_s(x) \exp(-iq_r x). \tag{19}$$

This result is interesting from two points of view. First, it significantly shortens the calculation time, because there are efficient procedures for calculating numerically Fourier transforms. Second, one can draw (directly from this formula) some physical conclusions about the influence of different elements of experimental scheme on the result.

In the case of nondispersive scheme, where $M = 1$, the consideration of the source sizes is reduced to application of a constant factor $G'_B(0)$. In other words, the source size affects in no way the DRC shape. When $M$ only slightly differs from unity, the curve of the source function is wide, therefore, the influence of the source is weak. If the difference is large, the source influence may be strong. Approximating the source intensity function $G_B(q_s)$ by a Gaussian

$$G_B(q_s) = \frac{1}{\sigma_s(2\pi)^{1/2}} \exp\left(-\frac{q_s^2}{2\sigma_s^2}\right), \tag{20}$$

one can calculate analytically $G'_B(x)$; the result is

$$G'_B(x) = \exp\left(-\frac{1}{2}\sigma_s^2 x^2\right). \tag{21}$$

It also follows from the obtained formula that, if the curve $G'_C(x)$ has a minimum FWHM among all four functions, an almost intrinsic DRC is obtained for the crystal sample as a result. If $G'_B(x)$ has a minimum FWHM, the experiment will yield the source angular size. Similarly, in the case of a very narrow slit, an experiment may yield the slit angular size. One can also obtain an almost intrinsic DRC of the monochromator.

The intrinsic DRCs of the monochromator and sample often have comparable widths, and the width of slit DRC may have either smaller or larger; a larger width is observed for a narrow slit. The slit angular width is defined as $\theta_S = \lambda/D$, where $D = 2x_0$ is the slit width. This result can be obtained directly from formula (14). At $\lambda = 10^{-10}$ m and $D = 50$ μm, $\theta_S = 2$ μrad. Even such a narrow slit should not lead to strong broadening of experimental DRC.

The above-considered approximation corresponds to the geometrical optics approximation for crystals. It is often used when analyzing the diffraction of divergent radiation in crystals, including deformed ones. Slits are often described in the same way.

Note that the function $G'_S(x)$ also has an analytical form:

$$G'_S(x) = 2x_0\left(1 - \frac{|x|}{2x_0}\right)\theta(2x_0 - |x|). \quad (22)$$

Formula (22) can easily be derived taking into account that this function is a convolution of two slit functions $\theta(x_0 - |x|)$. In other words, it is equal to the overlap area of two rectangles of unit height and width $2x_0$. This function amounts to $2x_0$ in the case of complete overlap, is zero (no overlap) when the rectangles are spaced by a distance of $2x_0$ or larger, and changes linearly between points 0 and $2x_0$.

## LIMITING CASE OF LARGE-SIZE SLIT

In this case, we obtain the following approximation for experimental DRC:

$$S(\theta_r) \propto \int \frac{dq_s}{2\pi} G_B(q_s) \int \frac{dq_1}{2\pi} \int \frac{dq}{2\pi} G_M(q - q_1) \times G_C(q_r + q_1 M - q) G_T(q - q_s), \quad (23)$$

where

$$G_T(q) = T(r^2 q) = \theta(x_0 - |r^2 q|). \quad (24)$$

As in the previous section, this triple integral can be reduced (by the Fourier transform method) to a single integral in the form

$$S(\theta_r) \propto \int dx G'_B([1 - M]x) G'_M(Mx) \times G'_T([1 - M]x) G'_C(x) \exp(-iq_r x). \quad (25)$$

The most important conclusion that follows from formula (25) is that the DRC shape is independent of the source sizes and slit size in the nondispersive scheme (where $M = 1$). It is determined by convolution of the monochromator and crystal sample DRCs. This property can easily be derived directly from formula (23) by replacing the variable $q_1$ with $q - q_1$ in the integral over $q_1$. The functions $G_M$ and $G_C$ cease to depend on $q$, and the integrals over $q_s$ and $q$ are transformed into factors independent of $q_r$.

It is of interest that the same conclusion follows from the formula presented in the previous section for a large-size slit. The source size again does not affect the DRC shape, and a wide slit leads to a large FWHM of the function $G'_S(x)$ in comparison with the FWHMs of the monochromator and crystal sample functions, $G'_M(x)$ and $G'_C(x)$, respectively.

However, the situation changes in the dispersion scheme, where $M$ differs from unity. Now one must take into account the function $G'_T(x)$, which has the form

$$G'_T(x) = \frac{1}{\pi x}\sin\left(\frac{x_0}{r^2}x\right). \quad (26)$$

The FWHM of this function is $\pi r^2/x_0$. It may become arbitrarily small with an increase in the slit width. Correspondingly, the DRC FWHM will be arbitrarily large and determined by only the angular divergence of radiation within a wide slit. In this case, the crystals affect only slightly the result.

## SPECIFIC EXAMPLES

When carrying out numerical calculations based on formulas (19) and (25), it is reasonable to use the functions $G'_B(x)$, $G'_M(x)$, $G'_S(x)$, and $G'_T(x)$ in normalization, when they are equal to unity for $x = 0$. In this case, they in no way distort the intrinsic DRC of crystal sample if their FWHM is very large in comparison with the intrinsic DRC. The main question of the theory is how these functions distort the shape of the intrinsic DRC of crystal sample.

Specific examples were calculated for the parameters of the "X-Ray Crystallography and Physical Materials Science" beamline of the Kurchatov SR source [17]: $l_0 = 13$ m; $\sigma_s = K\sigma_x/l_0$, where $\sigma_x = 54$ μm is a parameter of the Gaussian that models the source transverse size in real space; X-ray photon energy $E =$ 12 keV; and $K = 6.0812 \times 10^4$ μm$^{-1}$.

The computer program is written in ACL [18]. The DRAs $P_M(q)$ and $P_C(q)$ were calculated using a standard module for the general case of multilayer crystal, based on formulas [19]. One layer of sufficiently large thickness was used. The most interesting situation arises for the dispersion scheme with $M < 1$. Let us consider a silicon monochromator with a symmetric reflection 333 and a silicon crystal sample with a symmetric reflection 111. In this case, $\tan\theta_{B1} = 29.621°$, $\tan\theta_{B2} = 9.483°$, and $M = 0.2938$.

Fourier integrals were calculated by the fast Fourier transform (FFT) method on grids with a constant step and number of points $2^{16} = 65536$. The range of variation in argument $x$ was $X = 512$ μm. In correspondence with the FFT conditions, the grid step for argument $q$ was $2\pi/X$, with the same number of points. In fact, the functions change significantly in smaller intervals;

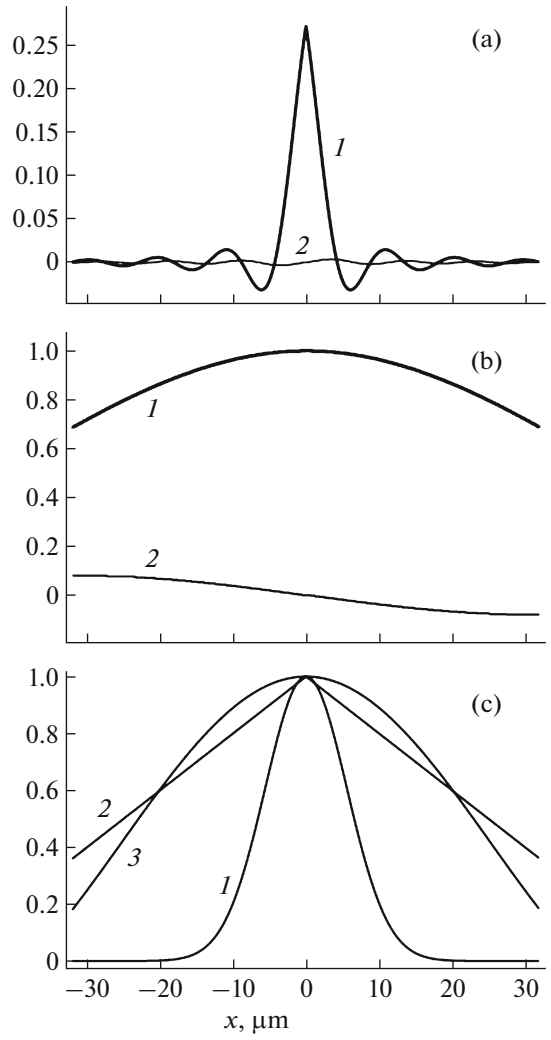


**Fig. 2.** Plots of the functions the convolution with which forms the experimental DRC: (a) the complex function $G'_C(x)$, the Fourier integral of which is equal to the intrinsic DRC of crystal sample ((*1*) real and (*2*) imaginary parts); (b) the complex function $G'_M(Mx)$, which describes the influence of the monochromator; and (c) the functions (*1*) $G'_B([1 - M]x)$, (*2*) $G'_S(x)$, and (*3*) $G'_T([1 - M]x)$.

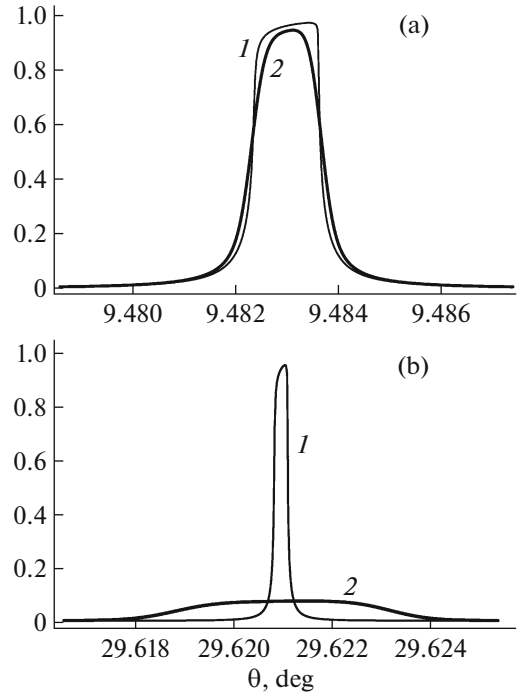


**Fig. 3.** Plots of the (*1*) intrinsic and (*2*) experimental DRCs for the reflections (a) 111 and (b) 333 in a Si sample (Si monochromator, 333).

therefore, not all points of grid but only its central part was used for plots.

Figure 2 shows the functions $G'_C(x)$, $G'_M(Mx)$, $G'_B([1 - M]x)$, $G'_S(x)$, and $G'_T([1 - M]x)$ for the aforementioned case and a slit width of 50 μm. The first two functions are complex and have a small imaginary part, because the corresponding Fourier transforms are asymmetric. They are shown in Figs. 2a and 2b by two curves, corresponding to the real and imaginary parts (curves *1* and 2, respectively). The other three functions, enumerated as *1*, *2*, and *3*, are presented in Fig. 2c

The first three functions are independent of the slit width; they are used in the same way in both approximations for slits of small and large sizes. One can easily see that the function $G'_C(x)$ has the smallest FWHM, whereas the functions $G'_S(x)$ and $G'_T([1 - M]x)$, although differing in shape, distort only slightly the intrinsic DRC of the crystal sample. Therefore, it is no surprise that the simulation of experimental DRC is practically the same in both approximations.

The calculation result is shown in Fig. 3a. Here, curve *1* corresponds to the intrinsic DRC of the crystal sample in the approximation of incident plane monochromatic wave, while curve *2* simulates the experimental result. In correspondence with the chosen normalization, the areas under the curves are equal. The result is shown for the approximation of small-size slit (the curves plotted in both approximations almost coincides and can hardly be distinguished).

A specific feature of these two approximations is that the slit distorts the experimental DRC only when has very small sizes (due to the diffraction of radiation from it, when the slit angular width $\theta_S = \lambda/D$ exceeds the angular width of the intrinsic DRC of crystal sample). The angular width of large-size slit is small, and this slit does not distort the result.

At the same time, the approximation of large-size slit takes into account its angular size, related to the divergence of the beam incident on it. The initial divergence is not limited, while the slit limits it (the smaller the slit size, the stronger this limitation is). As

a calculation shows, there is a range of sizes within which the slit does not distort the experimental DRC.

One can easily find that a slit of size $D = 1$ μm has an angular width $\lambda/D = 100$ μrad due to the diffraction. This value exceeds the angular width of intrinsic DRC; i.e., the width of the experimental DRC is approximately the same, and the second derivative differs from zero at the center. At the same time, a slit of size $D = 2$ mm has an angular width $D/l_0 = 154$ μrad. With allowance for the factor $(1 - M)$, the angular FWHM of experimental DRC is 109 μrad or 0.0062°, and the second derivative at the center is close to zero. These estimates are in complete agreement with the results of numerical calculations.

Let us consider the opposite situation: a monochromator with a 111 reflection and a crystal sample with a 333 reflection. In this case, the parameter $M = 3.404$, and the Bragg angles have the same values as in the previous case, but only interchange. Under these conditions, the FWHM of the function $G'_C(x)$ is larger, the FWHM of the function $G'_M(Mx)$ is many times smaller, and the convolution result is determined by only the monochromator.

The calculation result is shown in Fig. 3b. As previously, curve *1* corresponds to the intrinsic DRC, and curve *2* simulates the experimental DRC. It is of interest that the experimental curve, although being very strongly broadened, still remains asymmetric. This asymmetry is explained by the fact that this curve is in fact the broadened DRC of the monochromator. However, the normalization is chosen so as to equalize the areas under both curves; therefore, the maximum in the curve is smaller than in the monochromator DRC.

## CONCLUSIONS

It was theoretically shown that the new scheme of two-beam X-ray diffraction using synchrotron radiation, composed of a monochromator with symmetric reflections, a narrow slit, and a crystal sample, makes it possible to obtain almost intrinsic DRC of crystal sample. To this end, one must apply a monochromator with reflections at a large Bragg angle, exceeding the Bragg angle for the crystal sample by a factor of 2 or more.

In this case, the slit size should be optimized, because at a very small size possible X-ray diffraction from the slit increases the beam angular divergence, while at a large slit size the angular divergence of the initial beam may be anomalously large. The optimal value for a silicon crystal is 50 μm.

In the opposite case, the monochromator does not provide desired beam collimation and monochromatization, and the DRC of crystal sample is strongly broadened; the situation cannot be repaired by choosing an appropriate slit size. Thus, this scheme is valid for studying reflections with high Miller indices only when using a monochromator with reflections having very high indices.

The theory takes into account all parameters of the experimental scheme, including the source size, the distances between elements, and the slit size. It made it possible to explain the specific features of the experimental results obtained in [7, 9].

## ACKNOWLEDGMENTS

I am grateful to P.A. Prosekov for the interest in the study and valuable remarks.

## REFERENCES

1. Z. G. Pinsker, *Dynamical Scattering of X-Rays in Crystals* (Springer, Berlin, 1978).
2. N. Kato and A. R. Lang, Acta Crystallogr. **12**, 787 (1959).
3. V. V. Aristov, V. G. Kohn, V. I. Polovinkina, and A. A. Snigirev, Phys. Status Solidi A **72**, 483 (1982).
4. N. Kato, Acta Crystallogr. **14**, 526 (1961); N. Kato, Acta Crystallogr. **14**, 627 (1961).
5. A. Boulle, O. Masson, R. Guinebretiere, et al., J. Appl. Crystallogr. **35**, 606 (2002).
6. A. Kazimirov and V. G. Kohn, Acta Crystallogr. A **66**, 451 (2010).
7. A. E. Blagov, M. V. Koval'chuk, V. G. Kohn, et al., J. Surf. Invest. **5**, 822 (2011).
8. A. E. Blagov, M. V. Koval'chuk, V. G. Kohn, et al., Crystallogr. Rep. **55** (1), 10 (2010).
9. V. G. Kohn, P. A. Prosekov, A. Yu. Seregin, et al., Crystallogr. Rep. **64**, 24 (2019).
10. V. M. Kaganer, B. Jenichen, and K. H. Ploog, J. Phys. D: Appl. Phys. **34**, 645 (2001).
11. A. Mikhalychev, A. Benediktovitch, T. Ulyanenkova, and A. Ulyanenkov, J. Appl. Crystallogr. **48**, 679 (2015).
12. M. Sanchez del Rio and R. J. Dejus, Proc. SPIE **8141**, 814115 (2011).
13. V. Kohn, I. Snigireva, and A. Snigirev, Opt. Commun. **198**, 293 (2001).
14. V. G. Kohn and A. Kazimirov, Phys. Rev. B **75**, 224119 (2007).
15. V. Kohn, I. Snigireva, and A. Snigirev, Phys. Rev. Lett. **85**, 2745 (2000).
16. A. M. Afanas'ev and V. G. Kon, Sov. Phys. Crystallogr. **22**, 355 (1977).
17. http://kcsni.nrcki.ru/pages/main/12016/12076/12083/index.shtml.
18. http://kohnvict.ucoz.ru/acl/acl.htm.
19. V. G. Kohn, Phys. Status Solidi B **231**, 132 (2002).

*Translated by Yu. Sin'kov*